Electron Density Measurements of High Density Plasmas Using Soft X-Ray Laser Interferometry

L. B. Da Silva, T. W. Barbee, Jr., R. Cauble, P. Celliers, D. Ciarlo, S. Libby, R. A. London, D. Matthews, S. Mrowka, J. C. Moreno, D. Ress, J. E. Trebes, A. S. Wan, and F. Weber

Lawrence Livermore National Laboratory, P.O. Box 808, Livermore, California 94550

(Received 22 February 1995)

We have developed and used for the first time a soft x-ray interferometer to probe a large laser-produced plasma with micron spatial resolutions. A neonlike yttrium x-ray laser operating at 155 Å was combined with a multilayer coated Mach-Zehnder interferometer to obtain electron density profiles in a plasma produced by laser irradiation of a CH target. The measured electron density profile has been compared to hydrodynamic simulations and shows good agreement near the ablation surface but some discrepancy exists at lower densities.

PACS numbers: 52.70.La, 42.55.Vc, 52.25.Nr, 52.50.Jm

In the study of laser produced plasmas optical interferometry has played a key role in the accurate measurements of electron density profiles for a variety of target conditions. Profile steepening due to radiation pressure was first quantified by Attwood *et al.* [1] using a short pulse 2650 Å optical interferometer. It has been used to measure electron density profiles in exploding foils under conditions relevant to x-ray lasers [2,3]. The filamentation instability in laser produced plasmas was investigated by Young and co-workers [4,5] also using optical interferometry. In all these cases, however, the size of the plasma and the peak electron density accessible were severely restricted by absorption and refraction. In laser produced plasmas, inverse bremsstrahlung absorption becomes significant for optical probes at electron densities exceeding 10^{20} cm^{-3}. Refraction of the probe beam is sensitive to electron density gradients and ultimately affects spatial resolution and data interpretation [6]. These problems are particularly significant as we push forward to producing and studying large (3 mm) and high density plasmas (10^{22} cm^{-3}) relevant to inertial confinement fusion (ICF) [7] and astrophysics [8]. For these reasons there has existed a need to develop interferometry techniques at soft x-ray wavelengths where these effects can be mitigated. In this paper we describe the first use of interferometry at soft x-ray wavelengths to probe a laser produced plasma. We have combined a soft x-ray laser operating at 155 Å and a multilayer-optic-based interferometer to probe a mm size CH plasma. The electron density profile has been measured up to a density of 3×10^{21} cm^{-3}.

In a plasma with electron density n_e, the index of refraction n_{ref} is related to the critical electron density, $n_{\text{cr}} = 1.1 \times 10^{21} \lambda^{-2} [\text{cm}^{-3}]$ (λ in μm), by $n_{\text{ref}} = \sqrt{1 - n_e/n_{\text{cr}}}$. In an interferometer the number of fringe shifts, N_{fringe}, is then given by

$$N_{\text{fringe}} = \frac{\delta\phi}{2\pi} = \frac{1}{\lambda}\int_0^L (1 - n_{\text{ref}})\, dl \approx \frac{n_e}{2n_{\text{cr}}}\frac{L}{\lambda},$$

where the integral is along ray trajectories through the plasma, dL is the differential path length, L is the plasma length and we assume refraction effects are negligible. Experimentally, the maximum number of fringe shifts measurable is usually constrained by detector resolution and is rarely greater than ~50. This imposes a constraint on the product $n_e L$ for a given wavelength. An additional constraint which limits the accessible density and length parameter space is absorption. In a plasma dominated by free-free absorption the absorption coefficient α is given approximately by [9]

$$\alpha \approx 2.44 \times 10^{-37} \frac{\langle Z^2 \rangle n_e n_i}{\sqrt{kT}\,(h\nu)^3}\left[1 - \exp\left(\frac{-h\nu}{kT}\right)\right] \text{cm}^{-1}, \quad (1)$$

where the electron temperature kT and photon energy $h\nu$ are in eV and electron and ion densities are in cm^{-3}. The strong scaling with photon energy shows the advantage of probing with soft x-ray sources. For most high temperature plasmas of interest, the level of ionization is sufficient to eliminate any bound-free absorption in the soft x-ray region. Resonant line absorption is possible but very unlikely given the narrow bandwidth of the x-ray laser, ~10 mÅ [10]. Therefore, if we consider only free-free absorption in a plasma with 1 keV temperature and average ionization 30 (mid-Z plasma) we obtain from Eq. (1), $\alpha \approx 2.6 \times 10^{-43} n_e^2$ for $\lambda = 155$ Å. If we allow for one optical depth (i.e., $\alpha L = 1$) of absorption we obtain $n_e^2 L = 3.8 \times 10^{42}$. In Fig. 1 we show the electron density and plasma dimension accessible with a soft x-ray laser source (155 Å) which is constrained by free-free absorption and a maximum of 50 fringe shifts. This parameter space easily covers all plasmas normally produced in the laboratory.

Extending conventional interferometric techniques into the soft x-ray range has been difficult because of the problems with designing optical systems which operate in the range 40–400 Å. Reflective or grating systems have been discussed in the literature and have been used successfully at 1246 Å [11]. A purely reflective Fresnel bimirror setup has been demonstrated by Svatos *et al.* [12] at 48 Å. Both of these techniques, however, lack some of the advantages of standard interferometer

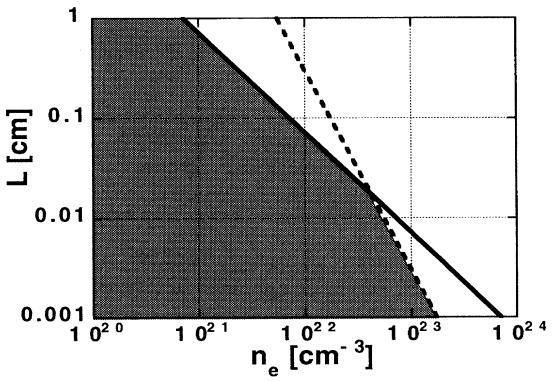

FIG. 1. The shaded area is the parameter space accessible for plasma probing using a soft x-ray laser (155 Å). The region is constrained by plasma absorption (dashed line) and the maximum fringe shifts allowed 50 (solid line).

geometries. Fortunately, multilayer mirror technology has now evolved to the point where artificial structures can be routinely fabricated with reflectivities as high as 65% at 130 Å [13,14] and with the overall uniformities required by more conventional interferometers.

The experimental setup used to probe plasmas is shown schematically in Fig. 2. The system consists of a collimated x-ray laser source, an imaging mirror, and an interferometer. For our experiments we chose to employ a skewed Mach-Zehnder interferometer consisting of two flat multilayer mirrors and two multilayer beam splitters. The polarizing properties of multilayer mirrors when operated at 45° prevented us from using a more conventional Mach-Zehnder geometry. Each multilayer mirror consisted of a superpolished (<1 Å rms roughness) fused silica blank coated with 30 layer pairs of 55.9 Å of Si and 23.9 Å of Mo. The mirrors were measured to have a peak reflectivity of (60 ± 5)% at 155 Å. The beam splitters used in the interferometer are the most critical element of the system. Soft x-ray beam splitters with small apertures have been previously used in x-ray laser cavities [15], but comparatively large open

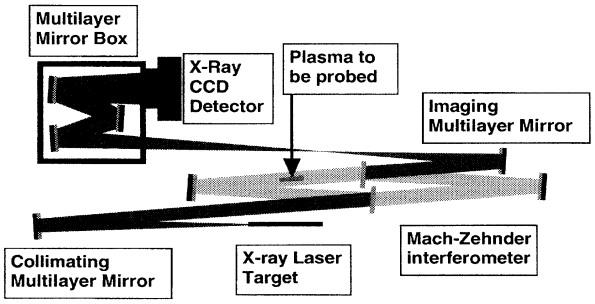

FIG. 2. Experimental setup showing the optical components for plasma probing using a soft x-ray Mach-Zehnder interferometer.

areas were necessary for our application. The *active* region of the beam splitters used in the interferometer was 1.2 cm × 1.2 cm and consisted of 1000 Å of silicon nitride overcoated with 8 to 12 layer pairs of Mo/Si. The beam splitters were fabricated from polished silicon wafers overcoated with 1000 Å of silicon nitride. The silicon substrate thickness was varied from 0.4 to 0.8 mm, with the best results being achieved with the thicker samples. The coated wafers were annealed to achieve maximum tension in the silicon nitride. Anisotropic silicon etching techniques were used to remove the silicon substrate from a 1.2 cm × 1.2 cm area. The flatness of the beam splitters was subsequently measured with an optical interferometer. Over the clear aperture the flatness was typically better than 5000 Å for high quality silicon substrates but could be significantly worse (10 000 Å) for conventional thin (0.4 mm) silicon wafers. The figure quality was also extremely sensitive to the tension of the silicon nitride membrane. The best results were obtained with high stress membranes (~200 MPa) which had a manufacturing yield of approximately 30%. The measured reflectivity and transmission for these beam splitters at 155 Å was 20% and 15%, respectively. The overall throughput of each arm, accounting for the mirror and beam splitter (one transmission and one reflection), was ~0.6 × 0.20 × 0.15 = 0.018.

A collisionally pumped neonlike yttrium x-ray laser operating at 155 Å was used as the probe source. The x-ray laser was produced by irradiating a solid 3 cm long yttrium target with one beam from Nova ($\lambda_{\text{laser}} = 0.53$ μm, 600 ps square) at an intensity of 1.5×10^{14} W/cm^2. The x-ray laser has an output energy of 3 ± 2 mJ, a divergence of approximately 10–15 mrad (FWHM), and an output pulse width of 350 ps. The short pulse and high brightness of the x-ray laser allowed us to obtain an interferogram in a single 350 ps exposure thereby reducing the effects of vibrations. A spherical multilayer mirror placed 50 cm from the x-ray laser was used to collimate the beam and inject it into the interferometer. The transverse coherence length after beam collimation was calculated to be $L_s \approx 50-100$ μm and the longitudinal coherence length is measured to be $L_t \approx 150$ μm. The limited transverse and longitudinal coherence constrains us to match the two paths of the interferometer to maximize fringe visibility. The interferometer was prealigned on an optical bench using a 100 μm optical fiber and a white light source. Observation of white light fringes was used to match the optical path lengths to better than 2 μm.

The plasma to be probed was imaged onto a charge coupled device (CCD) with a 100 cm radius of curvature multilayer mirror with an effective $f/\# = 25$. The CCD was a back illuminated TEK1024B with 1024 by 1024 24 μm pixels and a measured quantum efficiency of (40 ± 10)% at 155 Å. A filter consisting of 1000 Å of Al and 2000 Å of lexan directly in front of the CCD eliminated stray optical light. In order to reduce

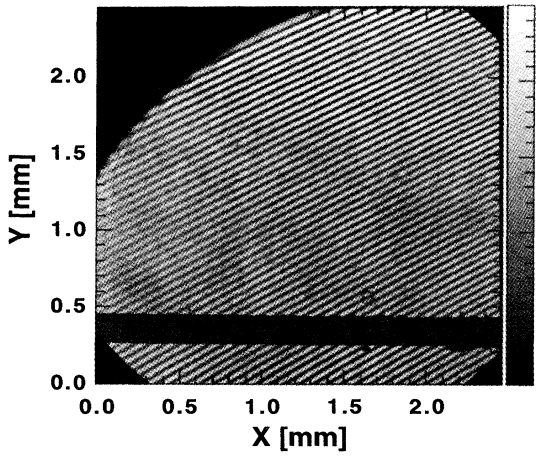

FIG. 3. Soft x-ray (155 Å) interferogram showing a fringe visibility better than 0.5. The horizontal bar is an alignment reference at the object plane.

background self-emission a series of three multilayer mirrors was used to reduce the bandpass of the system. The effective bandpass of this system was 4 Å, which is significantly broader than the 10 mÅ spectral width of the x-ray laser source. The image magnification was 19, giving a pixel limited resolution of ~ 1.3 μm. In Fig. 3 we show a typical interferogram obtained using this system. In this figure there is no target plasma; the dark band is an alignment reference positioned at the object plane of the imaging optic. Analysis of the fringe pattern gives a maximum figure error of 300 Å over the full 3 mm field of view and a fringe visibility of 0.7 ± 0.2.

In Fig. 4 we show the interferogram of a plasma produced by irradiating a silicon wafer overcoated with 10 μm of CH. The target was in the shape of a triangle to allow a range of plasma lengths to be probed simultaneously. The silicon substrate was polished to ~ 7 Å rms roughness to produce a clean flat surface. The CH side was irradiated with a beam smoothed with random phase plates and segmented with wedges to produce a flat-top intensity distribution over a 0.7 mm diam spot [16]. A 1 ns square laser pulse with a wavelength of 0.53 μm produced an intensity on target of 2.7×10^{13} W/cm^2. The target was backlit edge-on by the x-ray laser beam 1.1 ns after the start of the laser pulse. The image shows excellent fringe visibility and very little self-emission from the plasma.

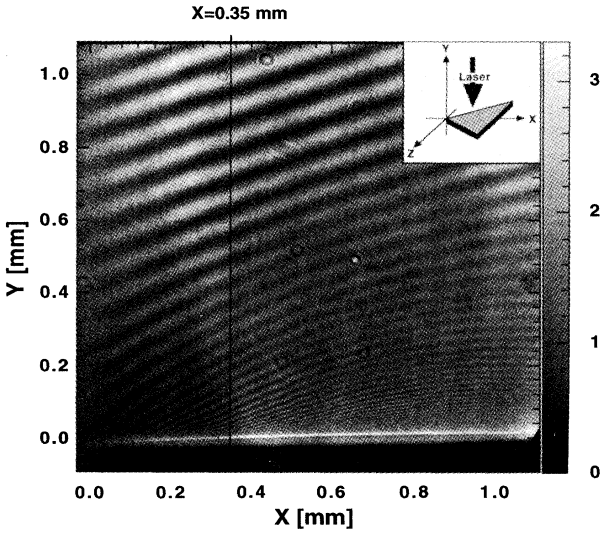

FIG. 4. Interferogram of CH target irradiated at 2.7×10^{13} W/cm^2. The inset shows the target geometry.

In Fig. 5 we show the measured electron density as calculated from the interferogram at a distance of 0.35 mm from the tip of the target where the probe length is 0.7 mm. Fringes are clearly resolved as close as 0.025 mm from the initial target surface. The fast evolution of the density profile close to the critical surface causes motion blurring of the fringes within the 350 ps x-ray laser frame time. Also shown in Fig. 5 is the calculated electron density profiles obtained from a one-dimensional LASNEX [17] simulation. The simulation results predict higher electron densities than measured with the discrepancy increasing as we move away from the surface. This trend is consistent with the plasma expansion not being one dimensional leading to significant lateral expansion and lower electron densities. We chose a triangular target geometry to illustrate the range of plasma lengths that can be easily probed with a soft x-ray laser but this leads to a three-dimensional expansion which is difficult to simulate. In the near term we plan to improve both the target geometry and laser uniformity to generate a truly two-dimensional profile which can be accurately compared to simulations. It is interesting to note, however, that the magnitude of the discrepancy we observed between the experiment and simulations is similar to that measured using soft x-ray deflectometry [18].

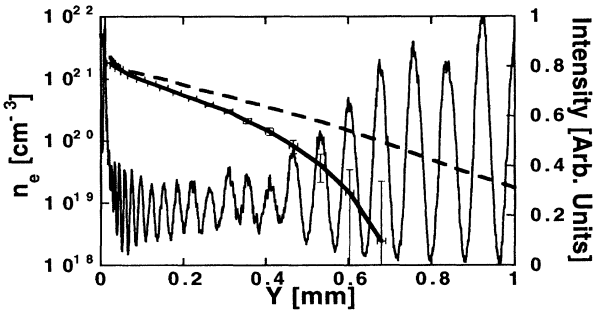

FIG. 5. The thin solid line is a lineout through the interferogram of Fig. 4 at a position $x = 0.35$ mm. The thick solid line shows the calculated electron density profile and estimated error bars. The dashed line is the electron density profile as calculated by one-dimensional LASNEX simulation.

The results presented in this paper illustrate the important role soft x-ray interferometry can play in diagnosing laser produced plasmas. Detailed comparisons of two-dimensional electron density profiles obtained from the x-ray laser interferogram and profiles obtained from radiation hydrodynamics codes, such as LASNEX, will allow us to study the physics of laser-plasma interactions in more detail. The ultimate motivation of the development of x-ray laser interferometry is to provide a mechanism to probe the deficiencies of our numerical model, in areas such as laser deposition by both resonance and inverse bremsstrahlung absorption, flux-limited heat conduction, hydrodynamics, and nonlocal thermodynamic equilibrium atomic kinetics. Aside from probing laboratory plasmas, the development of an xuv interferometer can play an important role in a variety of areas. For example, it can be used to characterize the figure and phase properties of multilayer mirrors near the intended operating wavelength. This is important because multilayer mirrors introduce a phase shift which is sensitive not only to the surface figure but also to the multilayer structure. This soft x-ray interferometer could also be used to measure spectral line shapes with resolutions far exceeding those currently possible [11,19].

We would like to thank Kent Estabrook for his help and suggestions regarding this work. We would also like to thank Jim Cox, Sharon Alvarez, Jeff Cardinal, Dennis Cocherell, Jeff Robinson, and the Nova Experiments Group for their assistance in these experiments. This work was performed under the auspices of the U.S. Department of Energy by the Lawrence Livermore National Laboratory under Contract No. W-7405-ENG-48.

[1] D. T. Attwood, D. W. Sweeney, J. M. Auerbach, and P. H. Y. Lee, Phys. Rev. Lett. **40**, 184 (1978).

[2] M. D. Rosen, P. L. Hagelstein, D. L. Matthews, E. M. Campbell, A. U. Hazi, B. L. Whitten, B. MacGowan, R. E. Turner, R. W. Lee, G. Charatis, G. E. Busch, C. L. Shepard, and P. D. Rockett, Phys. Rev. Lett. **54**, 106 (1985); G. Charatis, G. E. Busch, C. L. Shepard, P. M. Campbell, and M. D. Rosen, J. Phys. C **6**, 89 (1986).

[3] M. K. Prasad, K. G. Estabrook, J. A. Harte, R. S. Craxton, R. A. Bosch, G. E. Busch, and J. S. Kollin, Phys. Fluids B **4**, 1569 (1992).

[4] P. E. Young, Phys. Fluids B **3**, 2331–2336 (1991).

[5] S. Wilks, P. E. Young, J. Hammer, M. Tabak, and W. L. Kruer, Phys. Rev. Lett. **73**, 2994–2997 (1994).

[6] L. B. Da Silva, B. Cauble, G. Freiders, J. A. Koch, B. J. MacGowan, D. L. Matthews, S. Mrowka, D. B. Ress, J. E. Trebes, and T. L. Weiland, Proc. SPIE Int. Soc. Opt. Eng. **2012**, 158 (1994).

[7] B. G. Levi, Phys. Today **47**, No. 9, 17–19 (1994); M. D. Cable *et al.*, Phys. Rev. Lett. **73**, 2316 (1994); L. J. Suter *et al., ibid.* **73**, 2328 (1994); T. R. Dittrich *et al.. ibid.* **73**, 2324 (1994); R. L. Kauffman *et al., ibid.* **73**, 2320 (1994).

[8] T. S. Perry, S. J. Davidson, F. J. D. Serduke, D. R. Bach, C. C. Smith, J. M. Foster, R. J. Doyas, R. A. Ward, C. A. Iglesias, F. J. Rogers, J. J. Abdallah, R. E. Stewart, J. D. Kilkenny, and R. W. Lee, Phys. Rev. Lett. **67**, 3784 (1991); L. B. Da Silva, B. J. MacGowan, D. R. Kania, B. A. Hammel, C. A. Back, E. Hsieh, R. Doyas, C. A. Iglesias, F. J. Rogers, and R. W. Lee, Phys. Rev. Lett. **69**, 438 (1992).

[9] C. W. Allen, *Astrophysical Quantities* (Oxford University Press, New York, 1963), p. 100.

[10] J. Koch, B. J. MacGowan, L. B. D. Silva, D. L. Matthews, J. H. Underwood, P. J. Batson, and S. Mrowka, Phys. Rev. Lett. **68**, 3291 (1992).

[11] S. Chakrabarti, D. M. Cotton, J. S. Vickers, and B. C. Bush, Appl. Opt. **33**, 2596–2602 (1994).

[12] J. Svatos, D. Joyeux, D. Phalippou, and F. Polack, Opt. Lett. **18**, 1367 (1993).

[13] T. W. Barbee Jr., J. C. Rife, W. R. Hunter, M. P. Kowalski, R. G. Cruddace, and J. F. Seely, Appl. Opt. **32**, 4852–4854 (1993).

[14] D. G. Stearns, R. S. Rosen, and S. P. Vernon, J. Vac. Sci. Technol. A **9**, 2662–2669 (1991).

[15] A. M. Hawryluk, N. M. Ceglio, D. G. Stearns, K. Danzmann, M. Kühne, P. Müller, and B. Wende, Proc. SPIE Int. Soc. Opt. Eng. **688**, 81–90 (1987).

[16] S. G. Glendinning, S. V. Wever, P. Bell, L. B. Da Silva, S. N. Dixit, M. A. Henesian, D. R. Kania, J. D. Kilkenny, H. T. Powell, R. J. Wallace, P. J. Wegner, J. P. Knauer, and C. P. Verdon, Phys. Rev. Lett. **69**, 1201–1204 (1992).

[17] G. B. Zimmerman and W. L. Kruer, Commun. Plasma Phys. **2**, 85 (1975).

[18] D. Ress, L. B. Da Silva, R. A. London, J. E. Trebes, S. Mrowka, R. J. Procassini, J. T. W. Barbee, and D. E. Lehr, Science **265**, 514 (1994).

[19] M. R. Howells, K. Frank, Z. Hussain, E. J. Moler, T. Reich, D. Möller, and D. A. Shirley, Lawrence Berkeley Laboratory Report No. LBL-34798, 1993.

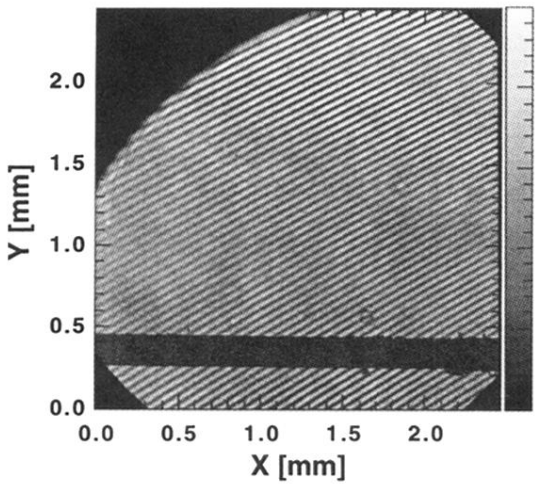

FIG. 3. Soft x-ray (155 Å) interferogram showing a fringe visibility better than 0.5. The horizontal bar is an alignment reference at the object plane.

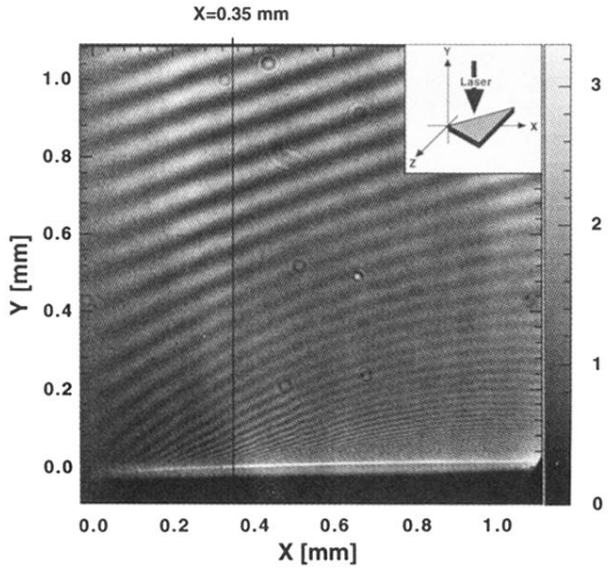

FIG. 4. Interferogram of CH target irradiated at 2.7×10^{13} W/cm^2. The inset shows the target geometry.